Search for Third Generation Scalar Leptoquarks Decaying into τb

V. M. Abazov,[36] B. Abbott,[75] M. Abolins,[65] B. S. Acharya,[29] M. Adams,[51] T. Adams,[49] E. Aguilo,[6] M. Ahsan,[59] G. D. Alexeev,[36] G. Alkhazov,[40] A. Alton,[64,*] G. Alverson,[63] G. A. Alves,[2] M. Anastasoaie,[35] L. S. Ancu,[35] T. Andeen,[53] S. Anderson,[45] B. Andrieu,[17] M. S. Anzelc,[53] M. Aoki,[50] Y. Arnoud,[14] M. Arov,[60] M. Arthaud,[18] A. Askew,[49] B. Åsman,[41] A. C. S. Assis Jesus,[3] O. Atramentov,[49] C. Avila,[8] F. Badaud,[13] L. Bagby,[50] B. Baldin,[50] D. V. Bandurin,[59] P. Banerjee,[29] S. Banerjee,[29] E. Barberis,[63] A.-F. Barfuss,[15] P. Bargassa,[80] P. Baringer,[58] J. Barreto,[2] J. F. Bartlett,[50] U. Bassler,[18] D. Bauer,[43] S. Beale,[6] A. Bean,[58] M. Begalli,[3] M. Begel,[73] C. Belanger-Champagne,[41] L. Bellantoni,[50] A. Bellavance,[50] J. A. Benitez,[65] S. B. Beri,[27] G. Bernardi,[17] R. Bernhard,[23] I. Bertram,[42] M. Besançon,[18] R. Beuselinck,[43] V. A. Bezzubov,[39] P. C. Bhat,[50] V. Bhatnagar,[27] C. Biscarat,[20] G. Blazey,[52] F. Blekman,[43] S. Blessing,[49] D. Bloch,[19] K. Bloom,[67] A. Boehnlein,[50] D. Boline,[62] T. A. Bolton,[59] E. E. Boos,[38] G. Borissov,[42] T. Bose,[77] A. Brandt,[78] R. Brock,[65] G. Brooijmans,[70] A. Bross,[50] D. Brown,[81] X. B. Bu,[7] N. J. Buchanan,[49] D. Buchholz,[53] M. Buehler,[81] V. Buescher,[22] V. Bunichev,[38] S. Burdin,[42,†] T. H. Burnett,[82] C. P. Buszello,[43] J. M. Butler,[62] P. Calfayan,[25] S. Calvet,[16] J. Cammin,[71] W. Carvalho,[3] B. C. K. Casey,[50] H. Castilla-Valdez,[33] S. Chakrabarti,[18] D. Chakraborty,[52] K. Chan,[6] K. M. Chan,[55] A. Chandra,[48] F. Charles,[19,**] E. Cheu,[45] F. Chevallier,[14] D. K. Cho,[62] S. Choi,[32] B. Choudhary,[28] L. Christofek,[77] T. Christoudias,[43] S. Cihangir,[50] D. Claes,[67] J. Clutter,[58] M. Cooke,[80] W. E. Cooper,[50] M. Corcoran,[80] F. Couderc,[18] M.-C. Cousinou,[15] S. Crépé-Renaudin,[14] V. Cuplov,[59] D. Cutts,[77] M. Ćwiok,[30] H. da Motta,[2] A. Das,[45] G. Davies,[43] K. De,[78] S. J. de Jong,[35] E. De La Cruz-Burelo,[64] C. De Oliveira Martins,[3] J. D. Degenhardt,[64] F. Déliot,[18] M. Demarteau,[50] R. Demina,[71] D. Denisov,[50] S. P. Denisov,[39] S. Desai,[50] H. T. Diehl,[50] M. Diesburg,[50] A. Dominguez,[67] H. Dong,[72] L. V. Dudko,[38] L. Duflot,[16] S. R. Dugad,[29] D. Duggan,[49] A. Duperrin,[15] J. Dyer,[65] A. Dyshkant,[52] M. Eads,[67] D. Edmunds,[65] J. Ellison,[48] V. D. Elvira,[50] Y. Enari,[77] S. Eno,[61] P. Ermolov,[38,**] H. Evans,[54] A. Evdokimov,[73] V. N. Evdokimov,[39] A. V. Ferapontov,[59] T. Ferbel,[71] F. Fiedler,[24] F. Filthaut,[35] W. Fisher,[50] H. E. Fisk,[50] M. Fortner,[52] H. Fox,[42] S. Fu,[50] S. Fuess,[50] T. Gadfort,[70] C. F. Galea,[35] E. Gallas,[50] C. Garcia,[71] A. Garcia-Bellido,[82] V. Gavrilov,[37] P. Gay,[13] W. Geist,[19] D. Gelé,[19] C. E. Gerber,[51] Y. Gershtein,[49] D. Gillberg,[6] G. Ginther,[71] N. Gollub,[41] B. Gómez,[8] A. Goussiou,[82] P. D. Grannis,[72] H. Greenlee,[50] Z. D. Greenwood,[60] E. M. Gregores,[4] G. Grenier,[20] Ph. Gris,[13] J.-F. Grivaz,[16] A. Grohsjean,[25] S. Grünendahl,[50] M. W. Grünewald,[30] F. Guo,[72] J. Guo,[72] G. Gutierrez,[50] P. Gutierrez,[75] A. Haas,[70] N. J. Hadley,[61] P. Haefner,[25] S. Hagopian,[49] J. Haley,[68] I. Hall,[65] R. E. Hall,[47] L. Han,[7] K. Harder,[44] A. Harel,[71] J. M. Hauptman,[57] R. Hauser,[65] J. Hays,[43] T. Hebbeker,[21] D. Hedin,[52] J. G. Hegeman,[34] A. P. Heinson,[48] U. Heintz,[62] C. Hensel,[22,§] K. Herner,[72] G. Hesketh,[63] M. D. Hildreth,[55] R. Hirosky,[81] J. D. Hobbs,[72] B. Hoeneisen,[12] H. Hoeth,[26] M. Hohlfeld,[22] S. Hossain,[75] P. Houben,[34] Y. Hu,[72] Z. Hubacek,[10] V. Hynek,[9] I. Iashvili,[69] R. Illingworth,[50] A. S. Ito,[50] S. Jabeen,[62] M. Jaffré,[16] S. Jain,[75] K. Jakobs,[23] C. Jarvis,[61] R. Jesik,[43] K. Johns,[45] C. Johnson,[70] M. Johnson,[50] A. Jonckheere,[50] P. Jonsson,[43] A. Juste,[50] E. Kajfasz,[15] J. M. Kalk,[60] D. Karmanov,[38] P. A. Kasper,[50] I. Katsanos,[70] D. Kau,[49] V. Kaushik,[78] R. Kehoe,[79] S. Kermiche,[15] N. Khalatyan,[50] A. Khanov,[76] A. Kharchilava,[69] Y. M. Kharzheev,[36] D. Khatidze,[70] T. J. Kim,[31] M. H. Kirby,[53] M. Kirsch,[21] B. Klima,[50] J. M. Kohli,[27] J.-P. Konrath,[23] A. V. Kozelov,[39] J. Kraus,[65] T. Kuhl,[24] A. Kumar,[69] A. Kupco,[11] T. Kurča,[20] V. A. Kuzmin,[38] J. Kvita,[9] F. Lacroix,[13] D. Lam,[55] S. Lammers,[70] G. Landsberg,[77] P. Lebrun,[20] W. M. Lee,[50] A. Leflat,[38] J. Lellouch,[17] J. Li,[78] L. Li,[48] Q. Z. Li,[50] S. M. Lietti,[5] J. G. R. Lima,[52] D. Lincoln,[50] J. Linnemann,[65] V. V. Lipaev,[39] R. Lipton,[50] Y. Liu,[7] Z. Liu,[6] A. Lobodenko,[40] M. Lokajicek,[11] P. Love,[42] H. J. Lubatti,[82] R. Luna,[3] A. L. Lyon,[50] A. K. A. Maciel,[2] D. Mackin,[80] R. J. Madaras,[46] P. Mättig,[26] C. Magass,[21] A. Magerkurth,[64] P. K. Mal,[82] H. B. Malbouisson,[3] S. Malik,[67] V. L. Malyshev,[36] H. S. Mao,[50] Y. Maravin,[59] B. Martin,[14] R. McCarthy,[72] A. Melnitchouk,[66] L. Mendoza,[8] P. G. Mercadante,[5] M. Merkin,[38] K. W. Merritt,[50] A. Meyer,[21] J. Meyer,[22,§] T. Millet,[20] J. Mitrevski,[70] R. K. Mommsen,[44] N. K. Mondal,[29] R. W. Moore,[6] T. Moulik,[58] G. S. Muanza,[20] M. Mulhearn,[70] O. Mundal,[22] L. Mundim,[3] E. Nagy,[15] M. Naimuddin,[50] M. Narain,[77] N. A. Naumann,[35] H. A. Neal,[64] J. P. Negret,[8] P. Neustroev,[40] H. Nilsen,[23] H. Nogima,[3] S. F. Novaes,[5] T. Nunnemann,[25] V. O'Dell,[50] D. C. O'Neil,[6] G. Obrant,[40] C. Ochando,[16] D. Onoprienko,[59] N. Oshima,[50] N. Osman,[43] J. Osta,[55] R. Otec,[10] G. J. Otero y Garzón,[50] M. Owen,[44] P. Padley,[80] M. Pangilinan,[77] N. Parashar,[56] S.-J. Park,[22,§] S. K. Park,[31] J. Parsons,[70] R. Partridge,[77] N. Parua,[54] A. Patwa,[73] G. Pawloski,[80] B. Penning,[23] M. Perfilov,[38] K. Peters,[44] Y. Peters,[26] P. Pétroff,[16] M. Petteni,[43] R. Piegaia,[1] J. Piper,[65] M.-A. Pleier,[22] P. L. M. Podesta-Lerma,[33,‡] V. M. Podstavkov,[50] Y. Pogorelov,[55] M.-E. Pol,[2] P. Polozov,[37] B. G. Pope,[65] A. V. Popov,[39] C. Potter,[6] W. L. Prado da Silva,[3] H. B. Prosper,[49] S. Protopopescu,[73] J. Qian,[64] A. Quadt,[22,§] B. Quinn,[66] A. Rakitine,[42] M. S. Rangel,[2] K. Ranjan,[28] P. N. Ratoff,[42] P. Renkel,[79] S. Reucroft,[63] P. Rich,[44] J. Rieger,[54] M. Rijssenbeek,[72] I. Ripp-Baudot,[19] F. Rizatdinova,[76] S. Robinson,[43] R. F. Rodrigues,[3]

M. Rominsky,[75] C. Royon,[18] P. Rubinov,[50] R. Ruchti,[55] G. Safronov,[37] G. Sajot,[14] A. Sánchez-Hernández,[33] M. P. Sanders,[17] B. Sanghi,[50] G. Savage,[50] L. Sawyer,[60] T. Scanlon,[43] D. Schaile,[25] R. D. Schamberger,[72] Y. Scheglov,[40] H. Schellman,[53] T. Schliephake,[26] C. Schwanenberger,[44] A. Schwartzman,[68] R. Schwienhorst,[65] J. Sekaric,[49] H. Severini,[75] E. Shabalina,[51] M. Shamim,[59] V. Shary,[18] A. A. Shchukin,[39] R. K. Shivpuri,[28] V. Siccardi,[19] V. Simak,[10] V. Sirotenko,[50] P. Skubic,[75] P. Slattery,[71] D. Smirnov,[55] G. R. Snow,[67] J. Snow,[74] S. Snyder,[73] S. Söldner-Rembold,[44] L. Sonnenschein,[17] A. Sopczak,[42] M. Sosebee,[78] K. Soustruznik,[9] B. Spurlock,[78] J. Stark,[14] J. Steele,[60] V. Stolin,[37] D. A. Stoyanova,[39] J. Strandberg,[64] S. Strandberg,[41] M. A. Strang,[69] E. Strauss,[72] M. Strauss,[75] R. Ströhmer,[25] D. Strom,[53] L. Stutte,[50] S. Sumowidagdo,[49] P. Svoisky,[55] A. Sznajder,[3] P. Tamburello,[45] A. Tanasijczuk,[1] W. Taylor,[6] B. Tiller,[25] F. Tissandier,[13] M. Titov,[18] V. V. Tokmenin,[36] T. Toole,[61] I. Torchiani,[23] T. Trefzger,[24] D. Tsybychev,[72] B. Tuchming,[18] C. Tully,[68] P. M. Tuts,[70] R. Unalan,[65] L. Uvarov,[40] S. Uvarov,[40] S. Uzunyan,[52] B. Vachon,[6] P. J. van den Berg,[34] R. Van Kooten,[54] W. M. van Leeuwen,[34] N. Varelas,[51] E. W. Varnes,[45] I. A. Vasilyev,[39] M. Vaupel,[26] P. Verdier,[20] L. S. Vertogradov,[36] M. Verzocchi,[50] F. Villeneuve-Seguier,[43] P. Vint,[43] P. Vokac,[10] E. Von Toerne,[59] M. Voutilainen,[68,‖] R. Wagner,[68] H. D. Wahl,[49] L. Wang,[61] M. H. L. S. Wang,[50] J. Warchol,[55] G. Watts,[82] M. Wayne,[55] G. Weber,[24] M. Weber,[50] L. Welty-Rieger,[54] A. Wenger,[23,¶] N. Wermes,[22] M. Wetstein,[61] A. White,[78] D. Wicke,[26] G. W. Wilson,[58] S. J. Wimpenny,[48] M. Wobisch,[60] D. R. Wood,[63] T. R. Wyatt,[44] Y. Xie,[77] S. Yacoob,[53] R. Yamada,[50] T. Yasuda,[50] Y. A. Yatsunenko,[36] H. Yin,[7] K. Yip,[73] H. D. Yoo,[77] S. W. Youn,[53] J. Yu,[78] C. Zeitnitz,[26] T. Zhao,[82] B. Zhou,[64] J. Zhu,[72] M. Zielinski,[71] D. Zieminska,[54] A. Zieminski,[54,**] L. Zivkovic,[70] V. Zutshi,[52] and E. G. Zverev[38]

(D0 Collaboration)

[1]*Universidad de Buenos Aires, Buenos Aires, Argentina*
[2]*LAFEX, Centro Brasileiro de Pesquisas Físicas, Rio de Janeiro, Brazil*
[3]*Universidade do Estado do Rio de Janeiro, Rio de Janeiro, Brazil*
[4]*Universidade Federal do ABC, Santo André, Brazil*
[5]*Instituto de Física Teórica, Universidade Estadual Paulista, São Paulo, Brazil*
[6]*University of Alberta, Edmonton, Alberta, Canada,*
Simon Fraser University, Burnaby, British Columbia, Canada,
York University, Toronto, Ontario, Canada,
and McGill University, Montreal, Quebec, Canada
[7]*University of Science and Technology of China, Hefei, People's Republic of China*
[8]*Universidad de los Andes, Bogotá, Colombia*
[9]*Center for Particle Physics, Charles University, Prague, Czech Republic*
[10]*Czech Technical University, Prague, Czech Republic*
[11]*Center for Particle Physics, Institute of Physics, Academy of Sciences of the Czech Republic, Prague, Czech Republic*
[12]*Universidad San Francisco de Quito, Quito, Ecuador*
[13]*LPC, Univ Blaise Pascal, CNRS/IN2P3, Clermont, France*
[14]*LPSC, Université Joseph Fourier Grenoble 1, CNRS/IN2P3, Institut National Polytechnique de Grenoble, France*
[15]*CPPM, Aix-Marseille Université, CNRS/IN2P3, Marseille, France*
[16]*LAL, Université Paris-Sud, IN2P3/CNRS, Orsay, France*
[17]*LPNHE, IN2P3/CNRS, Universités Paris VI and VII, Paris, France*
[18]*DAPNIA/Service de Physique des Particules, CEA, Saclay, France*
[19]*IPHC, Université Louis Pasteur et Université de Haute Alsace, CNRS/IN2P3, Strasbourg, France*
[20]*IPNL, Université Lyon 1, CNRS/IN2P3, Villeurbanne, France and Université de Lyon, Lyon, France*
[21]*III. Physikalisches Institut A, RWTH Aachen University, Aachen, Germany*
[22]*Physikalisches Institut, Universität Bonn, Bonn, Germany*
[23]*Physikalisches Institut, Universität Freiburg, Freiburg, Germany*
[24]*Institut für Physik, Universität Mainz, Mainz, Germany*
[25]*Ludwig-Maximilians-Universität München, München, Germany*
[26]*Fachbereich Physik, University of Wuppertal, Wuppertal, Germany*
[27]*Panjab University, Chandigarh, India*
[28]*Delhi University, Delhi, India*
[29]*Tata Institute of Fundamental Research, Mumbai, India*
[30]*University College Dublin, Dublin, Ireland*
[31]*Korea Detector Laboratory, Korea University, Seoul, Korea*
[32]*SungKyunKwan University, Suwon, Korea*
[33]*CINVESTAV, Mexico City, Mexico*
[34]*FOM-Institute NIKHEF and University of Amsterdam/NIKHEF, Amsterdam, The Netherlands*

[35]Radboud University Nijmegen/NIKHEF, Nijmegen, The Netherlands
[36]Joint Institute for Nuclear Research, Dubna, Russia
[37]Institute for Theoretical and Experimental Physics, Moscow, Russia
[38]Moscow State University, Moscow, Russia
[39]Institute for High Energy Physics, Protvino, Russia
[40]Petersburg Nuclear Physics Institute, St. Petersburg, Russia
[41]Lund University, Lund, Sweden, Royal Institute of Technology and Stockholm University, Stockholm, Sweden, and Uppsala University, Uppsala, Sweden
[42]Lancaster University, Lancaster, United Kingdom
[43]Imperial College, London, United Kingdom
[44]University of Manchester, Manchester, United Kingdom
[45]University of Arizona, Tucson, Arizona 85721, USA
[46]Lawrence Berkeley National Laboratory and University of California, Berkeley, California 94720, USA
[47]California State University, Fresno, California 93740, USA
[48]University of California, Riverside, California 92521, USA
[49]Florida State University, Tallahassee, Florida 32306, USA
[50]Fermi National Accelerator Laboratory, Batavia, Illinois 60510, USA
[51]University of Illinois at Chicago, Chicago, Illinois 60607, USA
[52]Northern Illinois University, DeKalb, Illinois 60115, USA
[53]Northwestern University, Evanston, Illinois 60208, USA
[54]Indiana University, Bloomington, Indiana 47405, USA
[55]University of Notre Dame, Notre Dame, Indiana 46556, USA
[56]Purdue University Calumet, Hammond, Indiana 46323, USA
[57]Iowa State University, Ames, Iowa 50011, USA
[58]University of Kansas, Lawrence, Kansas 66045, USA
[59]Kansas State University, Manhattan, Kansas 66506, USA
[60]Louisiana Tech University, Ruston, Louisiana 71272, USA
[61]University of Maryland, College Park, Maryland 20742, USA
[62]Boston University, Boston, Massachusetts 02215, USA
[63]Northeastern University, Boston, Massachusetts 02115, USA
[64]University of Michigan, Ann Arbor, Michigan 48109, USA
[65]Michigan State University, East Lansing, Michigan 48824, USA
[66]University of Mississippi, University, Mississippi 38677, USA
[67]University of Nebraska, Lincoln, Nebraska 68588, USA
[68]Princeton University, Princeton, New Jersey 08544, USA
[69]State University of New York, Buffalo, New York 14260, USA
[70]Columbia University, New York, New York 10027, USA
[71]University of Rochester, Rochester, New York 14627, USA
[72]State University of New York, Stony Brook, New York 11794, USA
[73]Brookhaven National Laboratory, Upton, New York 11973, USA
[74]Langston University, Langston, Oklahoma 73050, USA
[75]University of Oklahoma, Norman, Oklahoma 73019, USA
[76]Oklahoma State University, Stillwater, Oklahoma 74078, USA
[77]Brown University, Providence, Rhode Island 02912, USA
[78]University of Texas, Arlington, Texas 76019, USA
[79]Southern Methodist University, Dallas, Texas 75275, USA
[80]Rice University, Houston, Texas 77005, USA
[81]University of Virginia, Charlottesville, Virginia 22901, USA
[82]University of Washington, Seattle, Washington 98195, USA

(Received 21 June 2008; published 10 December 2008)

We have searched for third generation leptoquarks (LQ_3) using 1.05 fb^{-1} of data collected with the D0 detector at the Fermilab Tevatron Collider operating at $\sqrt{s} = 1.96$ TeV. We set a 95% C.L. lower limit of 210 GeV on the mass of a scalar LQ_3 state decaying solely to a b quark and a τ lepton.

DOI: 10.1103/PhysRevLett.101.241802 PACS numbers: 13.85.Rm, 14.80.−j

The standard model (SM) provides a good description of experimental data to date but fails to address the disparity between the electroweak scale and the much higher grand unification or Planck scale. Models invoking new strong coupling sectors [1], grand unification [2], superstrings [3], or quark-lepton compositeness [4] may alleviate this problem. In these models, new leptoquark particles (LQs) carrying both lepton number and color charge quantum

numbers may arise. The observed suppression of flavor changing neutral currents implies that a particular LQ state should couple only to quarks and leptons of the same fermion generation. Thus the third generation LQ (LQ_3) will decay only into a b or t quark and a τ or ν_τ, depending on the LQ_3 electric charge. At the Fermilab Tevatron $p\bar{p}$ Collider, leptoquarks can be pair-produced through gluon-gluon fusion and $q\bar{q}$ annihilation with standard QCD color interactions. The charge $4/3$ LQ_3 decays to $\tau^+\bar{b}$ with a branching ratio (BR) of 1, whereas the charge $2/3$ LQ_3 decays to $\tau^+ b$ with coupling constant β and to $\bar{\nu}_\tau t$ with coupling $(1-\beta)$ (and charge conjugates for $\overline{LQ_3}$ decays). For the $\bar{\nu}_\tau t$ decay, the BR $= (1-\beta) \times f_{\mathrm{PS}}$ is further suppressed by the phase space factor f_{PS} due to the large top quark mass.

In run II, the D0 Collaboration set a lower mass limit of 229 GeV [5] for the charge $1/3$ $LQ_3 \to \nu_\tau \bar{b}$. Here we present new limits on the mass of leptoquarks with charge $4/3$ with decays $LQ_3 \to \tau\bar{b}$ and charge $2/3$ with decays $LQ_3 \to \tau b$. The best previous limit for this channel is 153 GeV [6,7]. For pair production, both LQ_3 charge states lead to the final state $\tau^+\tau^- b\bar{b}$. We identify one of the τ leptons through its decay $\tau \to \mu\nu_\mu\nu_\tau$ and the other through its hadronic decays. The presence of jets from b quarks is signalled by tracks displaced from the primary vertex. The final state sought is thus two b jets, μ, τ, and missing transverse energy ($\not\!\!E_T$). The techniques developed here will have wider use in searches for supersymmetry and for the Higgs boson. In Ref. [6], this final state was used to search for R-parity-violating top squarks in the mass region below the top quark. In the higher mass region probed here, the top squark decays may include final state top quarks, and their analysis is beyond the scope of this Letter.

The D0 detector [8,9] has a central tracking volume with a silicon microstrip vertex detector (pseudorapidity coverage $|\eta| < 3$) and a scintillating fiber tracker ($|\eta| < 2.5$) within a 2 T solenoidal magnet, an uranium or liquid-argon calorimeter ($|\eta| < 4.2$), and a surrounding muon identification system ($|\eta| < 2$), with tracking chambers and scintillators before and after solid iron toroid magnets. Events are selected using a suite of triggers requiring either a single muon or a muon in association with jets. This analysis is performed using 1.05 fb^{-1} of data collected in run II.

Muon candidates are required to have hits in the muon system matched to a track candidate with $p_T > 15$ GeV and $|\eta| < 2$ and are required to extrapolate to within 1.5 cm of the reconstructed primary vertex along the beam axis. Cosmic ray muons are removed using the muon scintillation counter timing. Muon candidates are required to be isolated from nearby particles by requiring a calorimeter energy deposit of less than 2.5 GeV within a hollow cone of $0.1 < \mathcal{R} < 0.4$ centered on the muon direction and less than 2.5 GeV associated with tracks (excepting the muon track) within $\mathcal{R} < 0.5$. Here $\mathcal{R} = \sqrt{(\Delta\phi)^2 + (\Delta\eta)^2}$ is the distance in η-ϕ space between objects.

We identify three types of tau candidates motivated by the decays: (1) $\tau^\pm \to \pi^\pm\nu$, (2) $\tau^\pm \to \pi^\pm\pi^0\mathrm{s}\nu$, and (3) $\tau^\pm \to \pi^\pm\pi^\pm\pi^\mp(\pi^0\mathrm{s})\nu$. The corresponding selections [10] for the three types are based on tracks with transverse momenta $p_T^{\mathrm{trk}} > 1.5$ GeV and energy clusters in the electromagnetic (EM) calorimeter, both within a cone of $\mathcal{R} < 0.5$. The visible transverse momentum of a tau candidate p_T^τ is constructed from the calorimeter transverse energy (E_T^τ), corrected by track information where warranted. The tau selections are (1) a single isolated track with transverse momentum $p_T^{\mathrm{trk}} > 15$ GeV and no nearby electromagnetic energy cluster, (2) a single isolated track with $p_T^{\mathrm{trk}} > 7$ GeV with an associated EM cluster, and (3) two or more tracks, with at least one having $p_T^{\mathrm{trk}} > 7$ GeV, with or without associated EM clusters. Tau candidates must have p_T^τ above 15 GeV for types 1 and 2 and above 20 GeV for type 3. For type 1 candidates, we require $p_T^{\mathrm{trk}}/E_T^\tau \geq 0.7$ to reduce contributions from $\tau^\pm \to \pi^\pm\pi^0$'s in calorimeter regions with poor EM particle identification and $p_T^{\mathrm{trk}}/E_T^\tau \leq 2.0$ to reduce backgrounds from muons. A neural network [10] is formed for each τ type using input variables such as isolation and the transverse and longitudinal shower profiles of the calorimeter energy depositions associated with the tau candidate. The networks give an output variable $\mathcal{N}_i$ for τ-type i. We require $\mathcal{N}_1$, $\mathcal{N}_2$, and $\mathcal{N}_3$ to exceed 0.9, 0.9, and 0.95, respectively, corresponding to about 70% efficiency with $\geq 90\%$ rejection of fake jets.

We reconstruct jets using calorimeter energy deposits within a cone radius of 0.5 [11] and correct to the particle level using a jet energy scale correction (JES). Jets containing a muon are further corrected for the muon and average neutrino energies. Jets are required to have $p_T > 20$ GeV (>25 GeV for the highest p_T jet) and $|\eta| < 2.5$ relative to the center of the detector. We calculate $\not\!\!E_T$ from the transverse plane vector sum of calorimeter energy deposits, corrected for observed muons and for the jet and τ energy scale corrections.

We tag jets as b-jet candidates using a neural network algorithm [12] employing track impact parameters, significance of track displacement from the primary vertex, vertex mass, and number of tracks associated with a secondary vertex. The selection on the neural network output is optimized for the best LQ_3 sensitivity and has 72% efficiency for b jets, with a misidentification probability for light quark jets of 6%.

Events are preselected with the requirements that there is only one isolated muon and at least two jets with $\mathcal{R} > 0.5$ relative to the μ or τ candidates. If more than one τ candidate is found, the one with the largest p_T^τ is chosen. We require no electrons with $p_T > 12$ GeV.

The LQ_3 signal is simulated for $m_{LQ_3} = 120$–220 GeV in 20 GeV steps, using the PYTHIA [13] Monte Carlo (MC)

generator and CTEQ6L1 [14] parton distribution functions (PDFs). PYTHIA employs a leading order calculation [15,16] for scalar leptoquarks but does not include vector leptoquarks. The normalization at next-to-leading order (NLO) is taken from [17]. The $t\bar{t}$ and W/Z boson + jets backgrounds are simulated with the ALPGEN MC generator [18], with PYTHIA used for parton showering and fragmentation. The $t\bar{t}$ cross section is normalized to the next-to-next-to-leading order cross section [19] with top quark mass $m_t = 175$ GeV and the W/Z + jets cross sections are normalized to the W/Z inclusive NLO cross section [20]. The WW, WZ, and ZZ diboson backgrounds are generated using PYTHIA and normalized to the NLO cross sections [20]. The τ polarization and decays for all processes are simulated with TAUOLA [21]. The simulated events are processed through a GEANT [22] detector simulation and the standard D0 event reconstruction. They are further corrected for differences between data and MC simulation in the identification efficiencies for muons, electrons, and jets, Z boson p_T, the distribution of primary vertices along the beam axis, jet energy scale and resolution, b-jet tagging, and the effect of additional minimum bias interactions. The trigger efficiency applied to the simulated events is measured as a function of muon and jet azimuthal angle ϕ and η, respectively, and is appropriately averaged using the instantaneous luminosity in each data collection epoch.

We determine the multijet (MJ) background from two data samples, after subtracting the simulated SM backgrounds for both. The signal (SG) sample is that obtained from the preselected data discussed above. The enhanced background (BG) sample uses the preselection cuts, except that the muon track and calorimeter isolation requirements are reversed, and the τ identification requires $\mathcal{N}i < 0.8$. The shapes of the BG kinematic distributions agree well with those for the SG sample and provide the shape of the MJ background. We subdivide both SG and BG samples into opposite sign (OS) and same sign (SS) subsets according to whether the observed μ and τ charges are opposite or the same, with numbers of events N_C^Q ($C = \mathrm{SG}, \mathrm{BG}$, $Q = \mathrm{OS}, \mathrm{SS}$). The MJ background is computed as $N_{\mathrm{SG}}^{\mathrm{OS}} = f \times N_{\mathrm{SG}}^{\mathrm{SS}}$, where the MJ normalization factor is $f = N_{\mathrm{BG}}^{\mathrm{OS}}/N_{\mathrm{BG}}^{\mathrm{SS}}$. The factor f is observed to be close to 1 and independent of p_T^μ and p_T^τ. There is negligible LQ_3 signal in the SS BG subsample.

Further analysis uses the OS preselected events. Figure 1(a) shows the p_T distributions of the data and the sum of all backgrounds for the highest p_T jet. The agreement for this and other kinematic distributions is good. Figure 1(b) shows the data and background distributions for a variable related to the W boson mass, defined as $m^* = \sqrt{2E^\mu E^\nu(1 - \cos\Delta\phi)}$, where the estimated neutrino energy is $E^\nu = \not{E}_T(E^\mu/p_T^\mu)$ and $\Delta\phi$ is the azimuthal angle between the muon and $\not{E}_T$ directions. The $t\bar{t}$ and W + jets backgrounds contain a real W boson and have a high value of m^*, whereas the LQ_3 signal tends to have small m^*. Based on the expected LQ_3 mass limit from MC studies, we require $m^* < 60$ GeV.

The jets in the event sample after the m^* cut are subjected to the b-tagging algorithm, and subsets are formed with exactly one tagged b jet and with $\geq 2b$ jet tags. The numbers of events in the OS preselection sample, after the m^* requirement, and the 1 and ≥ 2 b-tagged jet subsamples, are shown in Table I.

We define the variable S_T as the scalar sum of the transverse momenta of μ, τ, the two highest p_T jets, and $\not{E}_T$. The LQ_3 signal is expected to have higher values of S_T than the background processes. Figure 1(c) shows the distributions of S_T for data and expected background, for the 1 b-tagged jet and ≥ 2 b-tagged jet samples combined. We observe no excess above the expected backgrounds.

The systematic uncertainty for the luminosity determination (6.1%) is taken from [23]. Calibration data sets are used to determine the uncertainties on the trigger efficiency (3%) and on the reconstruction, identification, and isolation efficiencies for the μ, τ, and jets (7%). The MC acceptance uncertainties due to the jet energy uncertainty are found to be 6%–9% by varying the JES by ± 1 standard deviation [24]. The uncertainties on the tagging rates for heavy flavor and light parton jets result in systematic

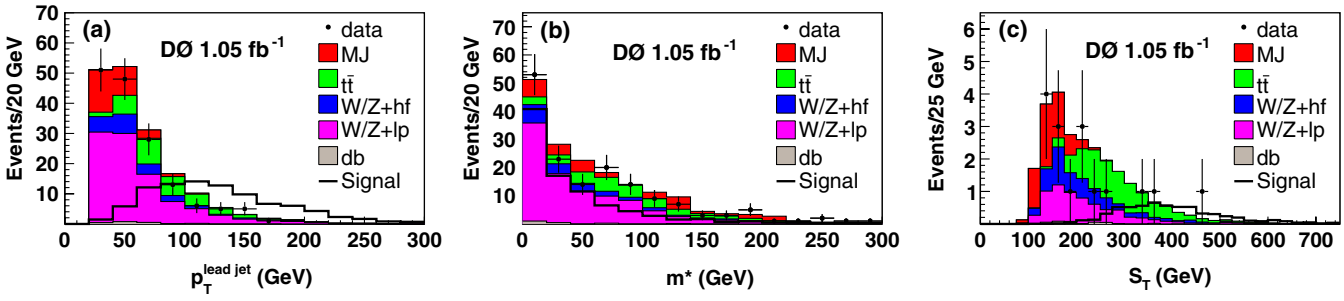

FIG. 1 (color online). Comparisons of data and the sum of backgrounds for (a) p_T of the highest p_T jet after preselection, (b) m^* after preselection, and (c) S_T for the 1 and ≥ 2 b tagged samples combined. We denote the diboson contribution as "db," heavy quarks (b, c) as "hf," and light partons (u, d, s, and gluons) as "lp." The LQ_3 signal is shown for $m_{\mathrm{LQ}_3} = 200$ GeV, multiplied by 10 in (a) and (b) and without scaling in (c).

TABLE I. Number of events for data and estimated backgrounds at the preselection level, after the m^* cut (before b-jet tagging), and for the 1 b-tag and ≥ 2 b-tag subsets. Light partons (u, d, s, g) are denoted as "lp." Also shown is the expected number of signal events for $m_{\mathrm{LQ}_3} = 200$ GeV. The uncertainties shown are statistical.

Source	Preselect	$m^* < 60$ GeV	1 b-tag	≥ 2 b-tag
W + lp	29.8 ± 1.8	11.2 ± 1.0	1.0 ± 0.4	<0.1
$W + c\bar{c}$	4.0 ± 0.4	1.5 ± 0.2	0.4 ± 0.1	<0.1
$W + b\bar{b}$	2.2 ± 0.2	0.8 ± 0.1	0.4 ± 0.1	<0.1
Z + lp	64.0 ± 0.7	55.3 ± 0.7	5.0 ± 0.2	0.1 ± 0.0
$Z + c\bar{c}$	8.3 ± 0.5	7.3 ± 0.5	1.7 ± 0.2	0.1 ± 0.1
$Z + b\bar{b}$	4.4 ± 0.2	3.8 ± 0.1	1.8 ± 0.1	0.4 ± 0.1
$t\bar{t}$	29.8 ± 0.3	10.6 ± 0.1	5.2 ± 0.1	3.1 ± 0.1
Diboson	2.0 ± 0.2	1.5 ± 0.1	0.3 ± 0.1	<0.1
MJ	25.2 ± 7.6	17.2 ± 5.6	4.0 ± 2.5	0.8 ± 1.0
Sum Bknd	169.6 ± 7.9	109.2 ± 5.7	19.6 ± 2.5	4.8 ± 1.0
Data	157	94	15	1
LQ pair signal	9.0 ± 0.2	7.4 ± 0.1	3.4 ± 0.1	2.6 ± 0.1

uncertainties on the signal acceptance (7.5%) and on the W/Z + heavy flavor jets background (7.5%) and W/Z + light parton jets background (15%) [12]. The MJ background uncertainty (15%) is determined by using independent MJ data samples in which either the μ isolation cuts or the τ neural network cuts (but not both) are reversed. The $t\bar{t}$ cross section uncertainty (18%) incorporates the estimated theoretical dependence on the renormalization and factorization scales [19], the uncertainty on m_t, and the uncertainty due to the PDF choice. The diboson production cross section uncertainty (6%) and the W/Z + jets cross section uncertainties (22%) are estimated using MCFM [20].

We compute the 95% C.L. upper limits on the signal cross section as a function of m_{LQ_3} using the modified frequentist method [25] as implemented in [26]. Negative log-likelihood ratio (LLR) test statistics are formed and combined from the S_T distributions for 1 and $\geq 2b$-tagged samples in simulated pseudoexperiments, under the background only (LLR_b) and signal plus background (LLR_{s+b}) hypotheses. We integrate LLR_b (LLR_{s+b}) above the LLR value observed in data to obtain confidence levels CL_b (CL_{s+b}). The LQ_3 cross section is varied until the ratio $\mathrm{CL}_s = \mathrm{CL}_{s+b}/\mathrm{CL}_b$ equals 0.05. The resulting expected and observed limits are shown in Fig. 2, together with the theoretical cross section (σ_{th}) assuming BR = 1. The observed cross section limit is within 1 standard deviation of the expected limit for $m_{\mathrm{LQ}_3} \approx 200$ GeV and within 2 standard deviations for all masses. The uncertainty on σ_{th} is obtained by varying renormalization and factorization scales by a factor of 2 above and below the central value of m_{LQ_3} and by taking into account the uncertainties in the PDFs [14,27]. The intersection of the observed cross section limit and the central σ_{th} as a function of m_{LQ_3} yields the exclusion of $m_{\mathrm{LQ}_3} > 210$ GeV (for $\beta = 1$), and at the 1 standard deviation lower value of σ_{th} we find $m_{\mathrm{LQ}_3} > 201$ GeV, both at the 95% C.L.

The dashed line in Fig. 2 indicates the decrease in the cross section $\times$ BR^2 for the charge 2/3 $\mathrm{LQ}_3 \rightarrow \tau b$ when the decay $\mathrm{LQ}_3 \rightarrow \nu_\tau t$ becomes kinematically possible, after including f_{PS} (for $\beta = 0.5$ and $m_t = 175$ GeV). In this case, we obtain $m_{\mathrm{LQ}_3} > 207$ GeV for the central σ_{th} and $m_{\mathrm{LQ}_3} > 201$ GeV for the 1 standard deviation lower limit of σ_{th}, at 95% C.L.

In summary, we have searched for third generation leptoquark pair production with decays $\mathrm{LQ}_3 \rightarrow \tau b$ and exclude $m_{\mathrm{LQ}_3} < 210$ GeV at the 95% C.L., assuming the branching fraction for this mode to be 1. This is the most

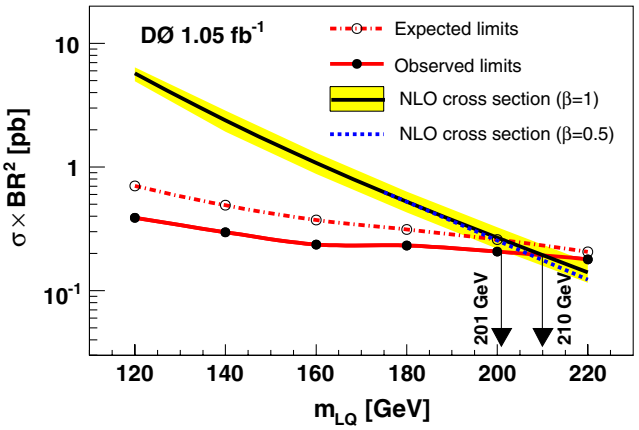

FIG. 2 (color online). Observed and expected cross section limits at the 95% C.L. of the pair production of third generation leptoquarks as a function of m_{LQ_3}. The uncertainty on the theoretical prediction is shown with shaded error bands. The theoretical cross section times branching ratio when $\beta = 1/2$ is shown as the dashed line.

stringent limit on third generation leptoquarks in this decay channel to date.

We thank the staffs at Fermilab and collaborating institutions and acknowledge support from the DOE and NSF (USA); CEA and CNRS/IN2P3 (France); FASI, Rosatom, and RFBR (Russia); CNPq, FAPERJ, FAPESP, and FUNDUNESP (Brazil); DAE and DST (India); Colciencias (Colombia); CONACyT (Mexico); KRF and KOSEF (Korea); CONICET and UBACyT (Argentina); FOM (The Netherlands); STFC (United Kingdom); MSMT and GACR (Czech Republic); CRC Program, CFI, NSERC, and WestGrid Project (Canada); BMBF and DFG (Germany); SFI (Ireland); The Swedish Research Council (Sweden); CAS and CNSF (China); and the Alexander von Humboldt Foundation (Germany).

[*]Visitor from Augustana College, Sioux Falls, SD, USA.
[†]Visitor from The University of Liverpool, Liverpool, United Kingdom.
[‡]Visitor from ICN-UNAM, Mexico City, Mexico.
[§]Visitor from II. Physikalisches Institut, Georg-August-University, Göttingen, Germany.
[‖]Visitor from Helsinki Institute of Physics, Helsinki, Finland.
[¶]Visitor from Universität Zürich, Zürich, Switzerland.
[**]Deceased.

[1] S. Dimopoulos and L. Susskind, Nucl. Phys. **B155**, 237 (1979); S. Dimopoulos, Nucl. Phys. **B168**, 69 (1980); E. Eichten and K. Lane, Phys. Lett. **90B**, 125 (1980).
[2] J. C. Pati and A. Salam, Phys. Rev. D **10**, 275 (1974); H. Georgi and S. L. Glashow, Phys. Rev. Lett. **32**, 438 (1974).
[3] J. L. Hewitt and T. G. Rizzo, Phys. Rep. **183**, 193 (1989).
[4] B. Schrempp and F. Schrempp, Phys. Lett. **153B**, 101 (1985); W. Buchmüller, R. Rückl, and D. Wyler, Phys. Lett. B **191**, 442 (1987); **448**, 320(E) (1999).
[5] V. M. Abazov *et al.* (D0 Collaboration), Phys. Rev. Lett. **99**, 061801 (2007).
[6] T. Aaltonen *et al.* (CDF Collaboration), Phys. Rev. Lett. **101**, 071802 (2008).
[7] G. Abbiendi *et al.* (OPAL Collaboration), Eur. Phys. J. C **31**, 281 (2003).
[8] S. Abachi *et al.* (D0 Collaboration), Nucl. Instrum. Methods Phys. Res., Sect. A **338**, 185 (1994).
[9] V. M. Abazov *et al.* (D0 Collaboration), Nucl. Instrum. Methods Phys. Res., Sect. A **565**, 463 (2006).
[10] V. M. Abazov *et al.* (D0 Collaboration), Phys. Rev. D **71**, 072004 (2005); **77**, 039901 (2008).
[11] G. C. Blazey *et al.*, Report No. FERMILAB-PUB-00-297, 2000.
[12] T. Scanlon, Report No. FERMILAB-THESIS-2006-43, 2006.
[13] T. Sjöstrand *et al.*, arXiv:hep-ph/030815; we use PYTHIA version 6.319.
[14] J. Pumplin *et al.*, J. High Energy Phys. 07 (2002) 012.
[15] J. L. Hewett and S. Pakvasa, Phys. Rev. D **37**, 3165 (1988).
[16] J. Blümlein, E. Boos, and A. Kryukov, Z. Phys. C **76**, 137 (1997).
[17] M. Kramer *et al.*, Phys. Rev. Lett. **79**, 341 (1997). This next-to-leading order calculation is for scalar, but not vector, leptoquarks.
[18] M. L. Mangano *et al.*, J. High Energy Phys. 07 (2003) 001; we use ALPGEN version 2.05.
[19] R. Bonciani *et al.*, Nucl. Phys. **B529**, 424 (1998); M. Cacciari *et al.*, J. High Energy Phys. 04 (2004) 068; N. Kidonakis and R. Vogt, Phys. Rev. D **68**, 114014 (2003).
[20] J. Campbell and R. K. Ellis, Phys. Rev. D **65**, 113007 (2002); we use MCFM version 3.4.5.
[21] S. Jadach *et al.*, Comput. Phys. Commun. **76**, 361 (1993).
[22] R. Brun and F. Carminati, CERN Program Library Long Writeup Report No. W5013, 1993.
[23] T. Andeen *et al.*, Report No. FERMILAB-TM-2365, 2007.
[24] V. M. Abazov *et al.* (D0 Collaboration), Phys. Rev. Lett. **101**, 062001 (2008).
[25] T. Junk, Nucl. Instrum. Methods Phys. Res., Sect. A **434**, 435 (1999).
[26] W. Fisher, Report No. FERMILAB-TM-2386-E, 2007.
[27] D. Stump *et al.*, J. High Energy Phys. 10 (2003) 046.